Analysis of Charge Order in the Kagome Metal AV3Sb5 (A=K,Rb,Cs)

Denner, M Michael ; Thomale, Ronny ; Neupert, Titus

Abstract: Motivated by the recent discovery of unconventional charge order, we develop a theory of electronically mediated charge density wave formation in the family of kagome metals AV3Sb5 (A=K,Rb,Cs). The intertwining of van Hove filling and sublattice interference suggests a three-fold charge density wave instability at TCDW. From there, the charge order forming below TCDW can unfold into a variety of phases capable of exhibiting orbital currents and nematicity. We develop a Ginzburg Landau formalism to stake out the parameter space of kagome charge order. We find a nematic chiral charge order to be energetically preferred, which shows tentative agreement with experimental evidence.

DOI: https://doi.org/10.1103/physrevlett.127.217601

Analysis of Charge Order in the Kagome Metal AV_3Sb_5 ($A = K, Rb, Cs$)

M. Michael Denner,[1] Ronny Thomale,[2,3] and Titus Neupert[1]
[1]Department of Physics, University of Zurich, Winterthurerstrasse 190, 8057 Zurich, Switzerland
[2]Institute for Theoretical Physics, University of Würzburg, Am Hubland, D-97074 Würzburg, Germany
[3]Department of Physics and Quantum Centers in Diamond and Emerging Materials (QuCenDiEM) group, Indian Institute of Technology Madras, Chennai 600036, India

(Received 2 April 2021; accepted 20 October 2021; published 19 November 2021)

Motivated by the recent discovery of unconventional charge order, we develop a theory of electronically mediated charge density wave formation in the family of kagome metals AV_3Sb_5 ($A = K, Rb, Cs$). The intertwining of van Hove filling and sublattice interference suggests a three-fold charge density wave instability at T_{CDW}. From there, the charge order forming below T_{CDW} can unfold into a variety of phases capable of exhibiting orbital currents and nematicity. We develop a Ginzburg Landau formalism to stake out the parameter space of kagome charge order. We find a nematic chiral charge order to be energetically preferred, which shows tentative agreement with experimental evidence.

DOI: 10.1103/PhysRevLett.127.217601

Introduction.—Density wave instabilities describe the onset of translation symmetry breaking of the charge or spin distribution in a Fermi liquid. While spin density waves usually unambiguously derive from electronic interactions, it is often subtle to tell whether electronic charge order is cause or consequence [1,2]. For the latter, structural transitions of any kind can accordingly manifest themselves in the rearranged electronic charge profile. For the former, the electron fluid minimizes its energy by translation symmetry breaking, which is mediated by electronic interactions. With regard to the charger order in the kagome metal AV_3Sb_5 ($A = K$, Rb, Cs) [3–12], a central observation to begin with is that it coincides with a Fermiology close to van Hove filling, hinting at a significant enhancement of electronic correlation effects. While it will still be essential to further analyse the phonon profile of the material [5,8], we take these observations to motivate our assumption that the supposed charge order observed in AV_3Sb_5 is electronically mediated, and that we will constrain ourselves to the electronic degrees of freedom in the following.

The kagome Hubbard model at van Hove filling has been predicted to yield a charge density wave (CDW) instability with finite angular momentum [13,14]. Generically, a charge density wave interpreted as a condensate of particle-hole singlets should tend to have zero angular momentum, in order for the particle hole pair to minimize its energy with respect to the screened Coulomb interactions. Instead, the van Hove-filling kagome Fermi surface yields three nesting vectors, all of which give rise to individual charge order components. Individually, the particle-hole pair wave function attains angular momentum $l = 1$, reminiscent of the generalization of the Peierls instability to two spatial dimensions also named charge bond order (CBO). The reason this instability is preferred over other instabilities roots in the sublattice interference [15], which effectively increases the relevance of nearest neighbor over on-site Coulomb repulsion within the nesting channels.

In this Letter, we develop a theory of charge order for AV_3Sb_5. In order to do so, we obtain an effective two-dimensional tight binding model which manages to keep the most salient features of the AV_3Sb_5 band structure. We find that, assuming an electronically mediated charge order, the Fermi pocket at van Hove filling should dominate. On a mean-field level, we compare CBO with $l = 1$ against charge density order (CDO) with $l = 0$ angular momentum, both for the same ordering wave vectors dictated by the Fermiology. We confirm that the threefold CBO instability previously found for the kagome Hubbard model at van Hove filling [13,14] dominates in a large part of parameter space. Beyond the instability level, the three CBO parameters can in principle form condensates which vary in amplitude and relative phase. We discuss the possibility using a Ginzburg Landau analysis and find that the CBO instability preferably breaks time-reversal symmetry. All three order parameters appear simultaneously at the instability level, and yet there is a tendency to nematicity through differing phases below T_{CDW}. These results appear to be in line with the measurements from scanning tunneling microscopy.

Multi-orbital effective model.—Layered kagome metals as the AV_3Sb_5 family are an exciting platform, hosting electronic features like flat bands and nodal lines [4,16]. The compounds can be treated as effectively two-dimensional [17], since the electronic features are dominated by the vanadium orbitals crystallizing in a kagome lattice structure. We now discuss the symmetry properties of bands arising from d orbitals in the kagome lattice, neglecting spin-orbit coupling. Located in the wallpaper group $p6mm$ (No. 17),

the kagome structure consists of three sublattices that arise from placing atoms on Wyckoff position $3g$ with site-symmetry group D_{2h}. The symmetry representations of Bloch states depend on the irreducible representation of the orbitals placed on these Wyckoff positions, as described by the topological quantum chemistry framework [18]. Two sets of orbitals contribute: First, a linear combination of the d_{xy}, $d_{x^2-y^2}$, d_{z^2} orbitals forms a Wannier state in the A_g irreducible representation of D_{2h}. We focus on the d_{xy} orbitals as their representative [see Fig. 1(a)]. They induce the well-known kagome band structure with a p-type van Hove singularity [19] at the M point [blue bands in Fig. 1(b)]. Second, the $d_{xz/yz}$ orbitals in the $B_{2g,3g}$ irreducible representations of D_{2h}, indicated as two red tones in Fig. 1(a), form a set of bands with opposite mirror eigenvalues along the Γ-M line. These bands give rise to a mirror-symmetry-protected Dirac cone on the Γ-M line and additional p- as well as m-type van Hove singularities [red bands in Fig. 1(b)]. Crossings between the d_{xy} and the $d_{xz/yz}$ bands are also protected by mirror symmetry.

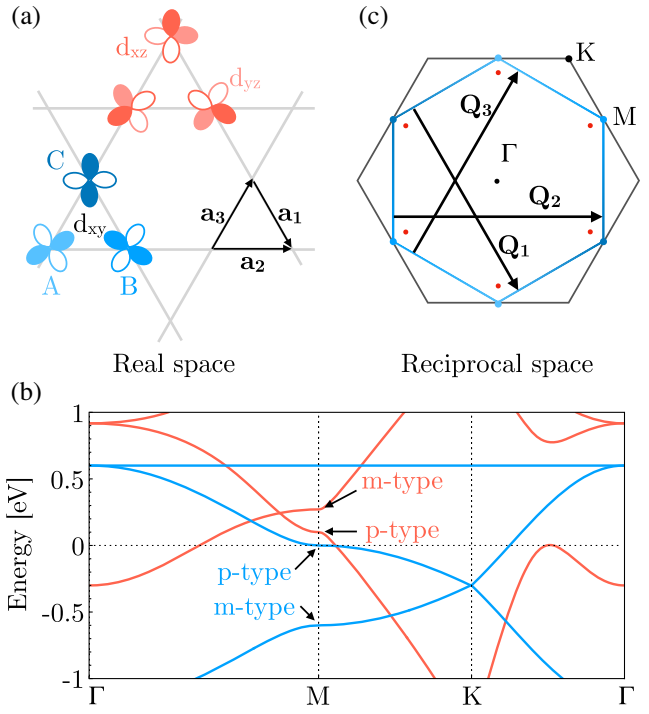

FIG. 1. Electronic features of AV_3Sb_5. (a) Kagome lattice with basis of three sublattices, occupied by vanadium d_{xy} (blue) and $d_{xz/yz}$ (red) orbitals. (b) Corresponding band structure induced by d_{xy} (blue) and $d_{xz/yz}$ (red) orbitals and corresponding nature of van Hove singularities. Higher-lying bands of $d_{xz/yz}$ are not displayed for simplicity. (c) Schematic of Fermi surfaces in the hexagonal Brillouin zone. The V d_{xy} Fermi surface, which is nested by the ordering wave vectors $\boldsymbol{Q}_j$, $j = 1, 2, 3$, has weight on distinct sublattices at each M point, giving rise to the sublattice interference mechanism. Dirac cones slightly above the Fermi energy are indicated in red according to their orbital origin.

P-type bands discussed above are subject to the sublattice interference [15]: at each M point, the Bloch states at van Hove filling have support on only one of the three sublattices [see Fig. 1(c)]. This effect is not an artifact of a simplified effective model, but is also seen in the first principles calculation to very high accuracy (corrected only by a small admixture from p orbtials of the other sublattices). It has a crucial influence on the character of Fermi instabilities [13,15,20].

In order to unravel the origin of the observed Fermi surface instability, we focus on nesting effects which are most apparent in the d_{xy} bands [see the nesting wave vectors $\boldsymbol{Q}_j$, $j = 1, 2, 3$, indicated in Fig. 1(c)]. We therefore focus on the d_{xy} orbitals exclusively in the following, while keeping in mind that $d_{xz/yz}$ bands share their important features—van Hove singularity and sublattice interference—and can thus be expected to support the ordering tendencies arising from the d_{xy} bands (see Sec. I in Ref. [21]).

The tight-binding description of the d_{xy} orbital band structure is $H_0 = \sum_{\boldsymbol{k},\alpha,\beta} c^\dagger_{\boldsymbol{k},\alpha} \mathcal{H}_{\boldsymbol{k},\alpha,\beta} c_{\boldsymbol{k},\beta}$, where $c^\dagger_{\boldsymbol{k},\alpha}$ creates a Bloch electron with momentum $\boldsymbol{k}$ in and support on sublattice $\alpha = 1, 2, 3$. The Bloch Hamiltonian matrix reads

$$\mathcal{H}_{\boldsymbol{k}} = -2t \begin{pmatrix} \mu & \cos(\boldsymbol{k}\boldsymbol{a}_3) & \cos(\boldsymbol{k}\boldsymbol{a}_2) \\ \cos(\boldsymbol{k}\boldsymbol{a}_3) & \mu & \cos(\boldsymbol{k}\boldsymbol{a}_1) \\ \cos(\boldsymbol{k}\boldsymbol{a}_2) & \cos(\boldsymbol{k}\boldsymbol{a}_1) & \mu \end{pmatrix}, \quad (1)$$

where we use the lattice vectors connecting sublattices as $\mathbf{a}_{1,3} = (1/4, \mp\sqrt{3}/4)^{\mathrm{T}}$, $\mathbf{a}_2 = (1/2, 0)^{\mathrm{T}}$, $t = 0.3$ eV as the overall hopping strength and μ as the chemical potential. The corresponding band structure presented in Fig. 1(b) shows an enhancement of the density of states around the three M points at the van Hove filling $n = 5/12$.

Charge density wave instability.—The emergence of the charge density wave in AV_3Sb_5 has been experimentally observed to break the translational symmetry of the kagome lattice to a 2×2 unit cell [4,6,8–12], thereby necessitating an instability with $\boldsymbol{Q} \neq 0$, specifically $\boldsymbol{Q}_{1,3} = (\pi, \mp\sqrt{3}\pi)^{\mathrm{T}}$, $\boldsymbol{Q}_2 = (2\pi, 0)^{\mathrm{T}}$ [see Fig. 1(c)]. Experimental evidence in AV_3Sb_5 is indicative of an electronically driven charge order [5,22]. This is why we consider a mean-field treatment of the kagome Hubbard model, realized by the Hamiltonian

$$\begin{aligned} H &= H_0 + H_{\mathrm{int}} \\ &= \mu \sum_{\boldsymbol{r},\sigma} c^\dagger_{\boldsymbol{r},\sigma} c_{\boldsymbol{r},\sigma} - t \sum_{\langle \boldsymbol{r},\boldsymbol{r}' \rangle,\sigma} (c^\dagger_{\boldsymbol{r},\sigma} c_{\boldsymbol{r}',\sigma} + \mathrm{H.c.}) \\ &\quad + U \sum_{\boldsymbol{r}} n_{\boldsymbol{r},\uparrow} n_{\boldsymbol{r},\downarrow} + V \sum_{\langle \boldsymbol{r},\boldsymbol{r}' \rangle,\sigma,\sigma'} n_{\boldsymbol{r},\sigma} n_{\boldsymbol{r}',\sigma'}, \end{aligned} \quad (2)$$

where $c^{\dagger}_{\boldsymbol{r},\sigma}$ creates an electron on site $\boldsymbol{r}$ in the kagome lattice with spin $\sigma = \uparrow, \downarrow$ and $n_{\boldsymbol{r},\sigma} = c^{\dagger}_{\boldsymbol{r},\sigma} c_{\boldsymbol{r},\sigma}$. The on-site Hubbard interaction is parametrized by U, while the nearest-neighbor interaction strength is denoted by V. Crucially, the hopping always acts between densities on sites belonging to different sublattices.

In the following, we only consider charge orders, i.e., all fermionic bilinear forms are implicitly summed over their spin degree of freedom. Note that a spin bond order with likewise finite relative angular momentum could, in principle, be a close competitor [13], which could evade conventional static measurements of local magnetic moments [23] and hence would not contradict, e.g., the absence of a local magnetic moment in μSR [24]. The current related to the anomalous Hall signal [25], however, manifestly is a charge current and not a spin current. Additionally, recent optical spectroscopy experiments support the bulk nature of the CDW state [9], and as such hint at an electronically mediated charge order as its origin.

The relative strength of on-site U and nearest neighbor V Hubbard interactions allow for different charge orders to emerge. Inspired by the majority of charge instabilities, a *charge density order* is an obvious possibility, described by the order parameter

$$\mathcal{O}_{\mathrm{CDO}}(\boldsymbol{k}) = \sum_{\alpha} \tilde{\Delta}_{\alpha} \langle c^{\dagger}_{\boldsymbol{k},\alpha} c_{\boldsymbol{k}+\boldsymbol{Q}_{\alpha},\alpha} \rangle, \tag{3}$$

where α labels the three sublattices. It corresponds to a real space pattern of the form

$$\mathcal{O}_{\mathrm{CDO}}(\boldsymbol{r}) = \sum_{\alpha} \tilde{\Delta}_{\alpha} \cos(\boldsymbol{Q}_{\alpha}\boldsymbol{R}) \langle c^{\dagger}_{\boldsymbol{R},\alpha} c_{\boldsymbol{R},\alpha} \rangle, \tag{4}$$

where $c^{\dagger}_{\boldsymbol{R},\alpha}$ creates an electron in sublattice α of unit cell $\boldsymbol{R}$, while $\boldsymbol{r} = \boldsymbol{R} + \boldsymbol{r}_{\alpha}$ is the actual position of the site ($\boldsymbol{r}_1 = \boldsymbol{0}$, $\boldsymbol{r}_2 = \boldsymbol{a}_3, \boldsymbol{r}_3 = \boldsymbol{a}_2$). Such an arrangement is visualized in the right inset of Fig. 2.

Owing to the unique sublattice structure, however, the inhomogeneous distribution of Fermi level density of states reduces nesting effects for a local Hubbard interaction. Consequently, the nearest-neighbor interaction V is promoted, leading to a *charge bond order*, which modulates the kinetic hopping strengths instead of on-site densities. Correspondingly, the order parameter in reciprocal space can be written as [13]

$$\mathcal{O}_{\mathrm{CBO}}(\boldsymbol{k}) = \sum_{\alpha,j,\beta} \Delta_j \sin\left(\frac{\boldsymbol{Q}_j \boldsymbol{k}}{4\pi}\right) \langle c^{\dagger}_{\boldsymbol{k},\alpha} c_{\boldsymbol{k}+\boldsymbol{Q}_j,\beta} \rangle |\epsilon_{\alpha j \beta}|, \tag{5}$$

where $\epsilon_{\alpha j \beta}$ is the Levi-Civita tensor and α, β run over the three sublattices. The $\boldsymbol{k}$ dependence of the order parameter creates a nontrivial relative momentum structure, leading to the formation of an unconventional CDW order. Note that the relative angular momentum $l = 1$ of the individual particle hole pairs does not directly carry over to the macroscopic charge order ground state formed by the coherent superposition of these particle hole pairs. Rather, the $l = 1$ substructure of the particle hole pair wave function unfolds in the nature of particle-hole excitations above the ground state. In real space, the emerging order corresponds to an alternating modulation of the hopping strengths connecting the three sublattices, giving rise to the enlarged 2×2 unit cell

$$\mathcal{O}_{\mathrm{CBO}}(\boldsymbol{r}) = \sum_{\alpha,j,\beta} \Delta_j \cos(\boldsymbol{Q}_j \boldsymbol{R}) |\epsilon_{\alpha j \beta}| \left(\langle c^{\dagger}_{\boldsymbol{R},\alpha} c_{\boldsymbol{R},\beta} \rangle - \langle c^{\dagger}_{\boldsymbol{R},\alpha} c_{\boldsymbol{R}-2\boldsymbol{a}_j,\beta} \rangle \right), \tag{6}$$

whose visualization is given in the left inset of Fig. 2. We compare the transition temperature of the two orders defined in Eqs. (3) and (5) on the mean-field level. The results are visualized in Fig. 2. Clearly, a CBO is favored for a wide range of interaction strengths, owing to the unique sublattice structure of the kagome lattice [27]. This allows nearest-neighbor interactions V to take the role of mediating the unconventional charge order. By contrast, the CDO is found in the limit of large on-site interaction U. Experimentally, a transition temperature $T_{\mathrm{CDW}} \approx 78$–$103$ K has been observed [6]. Gauging our scales from this input, it yields $U/2 = V \approx 250$ meV in our setting. Naturally, for sufficiently large on-site interactions U, the charge density order becomes dominant again, as seen on the right side of Fig. 2. Exerting hydrostatic pressure has been found to lead to a suppression of the charge

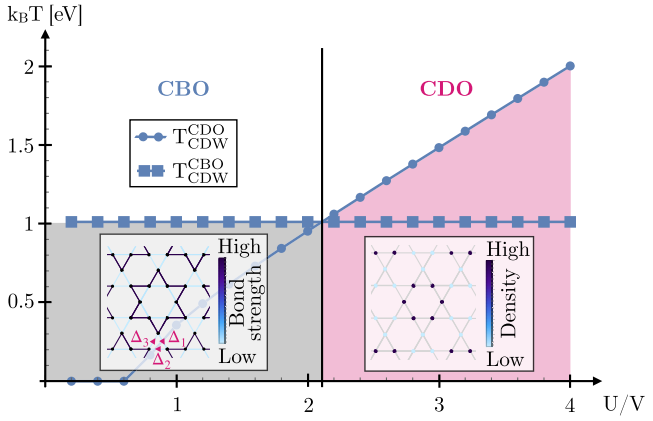

FIG. 2. Interaction strength phase diagram and corresponding electronic order in AV_3Sb_5. Mean field critical temperatures of the charge density order introduced in Eq. (3) and the charge bond order introduced in Eq. (5) as a function of the electronic interaction strengths U/V ($\mu = -35$ meV [26]). For $U \lesssim 2.1$ V a charge bond order dominates, which forms a complex star of David pattern of strong and weak bonds. The inset highlights the mean field parameters Δ_j, $j = 1, 2, 3$, and their arrangement on the kagome lattice. For systems with interaction scales above $U = 2.1$ V a charge density order emerges, modulating the real space site occupation.

order [10,26], related to both Fermi surface renormalizations and changes in the nearest-neighbor interaction V (see Sec. II in Ref. [21]).

Ginzburg Landau formalism.—To study the interplay of the triplet of order parameters in the CBO phase, we derive the symmetry-constrained expansion of the Ginzburg Landau free energy for Δ_1, Δ_2, Δ_3 as defined in Eq. (6). The relevant generating symmetries are translation by $2\boldsymbol{a}_1$, $(\Delta_1, \Delta_2, \Delta_3) \to (\Delta_1, -\Delta_2, -\Delta_3)$, translation by $2\boldsymbol{a}_2$, $(\Delta_1, \Delta_2, \Delta_3) \to (-\Delta_1, \Delta_2, -\Delta_3)$ six-fold rotation, $(\Delta_1, \Delta_2, \Delta_3) \to (\Delta_3^*, \Delta_1^*, \Delta_2^*)$, mirror with $\boldsymbol{a}_2$ normal to the mirror plane, $(\Delta_1, \Delta_2, \Delta_3) \to (\Delta_3^*, \Delta_2^*, \Delta_1^*)$, and time-reversal acting as complex conjugation. For a more compact notation, we decompose the complex order parameter into phase ϕ_j and absolute value $\psi_j > 0$ as $\Delta_j = \psi_j e^{i\phi_j}$, for $j = 1, 2, 3$. Up to third order in Δ_j, and neglecting gradient terms, the free energy expansion reads [29,30]

$$F = \alpha_1 \sum_j \psi_j^2 + 2\alpha_2 \sum_j \psi_j^2 \cos(2\phi_j) + 2\gamma_1 \psi_1\psi_2\psi_3 \cos(\phi_1 + \phi_2 + \phi_3) + \gamma_2 \psi_1\psi_2\psi_3 [8\cos(\phi_1)\cos(\phi_2)\cos(\phi_3) - 2\cos(\phi_1 + \phi_2 + \phi_3)], \tag{7}$$

with the coefficients $\alpha_{1,2}$ and $\gamma_{1,2}$ being temperature-dependent real numbers. We discuss the effect of the second- and third-order terms separately, with the vanishing $\alpha_1 \pm 2\alpha_2$ at T_{CDW} indicating the phase transition to the charge bond ordered state [see Fig. 3(a)].

The second order terms are minimized by $\phi_j \bmod \pi = 0$ for $\alpha_2 < 0$, and $\phi_j \bmod \pi = \pi/2$ for $\alpha_2 > 0$, where the latter case breaks time-reversal symmetry spontaneously and induces orbital currents [31,32]. Our microscopic calculation indeed yields $\alpha_2 > 0$, as seen in Fig. 3(a). The resulting bond correlation $\langle \psi_{\mathrm{GS}} | c_{\boldsymbol{r}}^\dagger c_{\boldsymbol{r}'} | \psi_{\mathrm{GS}} \rangle$, with $\boldsymbol{r}$, $\boldsymbol{r}'$ being nearest-neighbor sites and ψ_{GS} the single Slater determinant ground state wave function, replicates the expected star of David pattern imprinted by the modulated hopping elements. Additionally, orbital currents emerge due to the time-reversal symmetry breaking and, even though we have a bond order, the on-site densities $\langle \psi_{\mathrm{GS}} | c_{\boldsymbol{r}}^\dagger c_{\boldsymbol{r}} | \psi_{\mathrm{GS}} \rangle$ are also modulated [see Fig. 3(b)].

The third order terms in Eq. (7) mediate interactions between the three order parameters. They demonstrate that the simultaneous nucleation of all three order parameters is energetically favorable. Our microscopic calculation yields $\gamma_1 < 0$ and $\gamma_2 = 0$. Minimization of the third order terms alone then implies $\phi_1 + \phi_2 + \phi_3 \bmod 2\pi = 0$, which forces the ϕ_j to deviate from $\pm\pi/2$, while maintaining the time-reversal symmetry breaking. This competition between second and third order terms, together with the fourth order, leads to a transition from an isotropic to an anisotropic charge order upon lowering temperature. Specifically, a difference between the phase factors $\phi_1 \neq \phi_{2,3} \neq \pi/2$ emerges within the charge order phase, while maintaining a complex order parameter with $\psi_1 = \psi_2 = \psi_3$. This results in a *nematic* chiral charge order, where the bond correlations spontaneously break the C_6-rotational symmetry (see Sec. III in Ref. [21]). Such a scenario has been observed in numerous experiments [4,33–35].

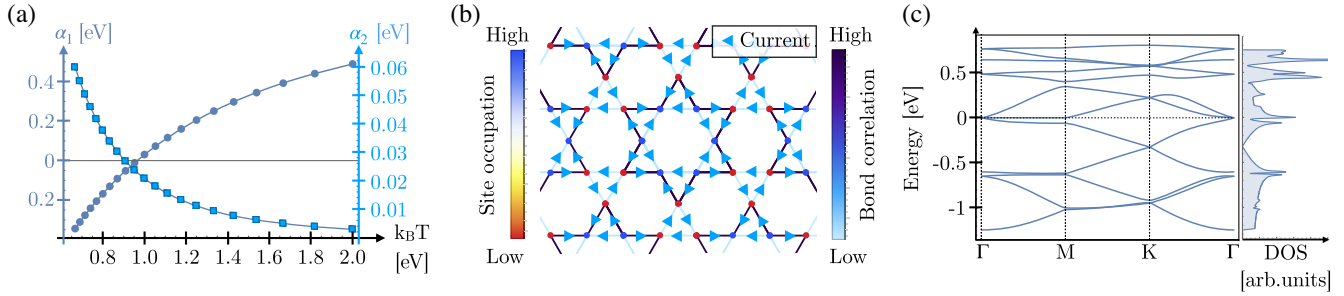

FIG. 3. Ginzburg Landau free energy and resulting current pattern. (a) The second order coefficient α_1 as a function of temperature T signals the second order phase transition of the emerging charge bond order by a sign change at $k_B T_{\mathrm{CDW}} \approx 1.011$ eV, whereas the coefficient α_2 is purely positive, requiring an imaginary order parameter Δ_j, breaking time-reversal symmetry ($V = 1$ eV, $\mu = -35$ meV). (b) The bond correlation pattern $\langle \psi_{\mathrm{GS}} | c_{\boldsymbol{r}}^\dagger c_{\boldsymbol{r}'} | \psi_{\mathrm{GS}} \rangle$ in this setting ($\Delta_j = 0.1\mathrm{i}$) shows a star of David arrangement of strong and weak bonds, equipped with a nonzero current. The current is homogeneous on the lattice, however alternating in its flow, indicated with blue arrows. Additionally, the order parameter modulates the on-site occupation within and between the hexagons. (c) The resulting band structure in the reduced Brillouin zone shows a gap opening around the M points, reducing the density of states (DOS) at the Fermi level ($\Delta_j = 0.1\mathrm{i}$).

We conclude from this Ginzburg Landau analysis three points that are in accordance with the experimental findings, in particular in AV_3Sb_5: (i) the CBO breaks time-reversal symmetry spontaneously, (ii) all three order parameter components nucleate together, and (iii) their competition can result in a nematic CBO.

In Fig. 3(c) the band structure of the time-reversal symmetry breaking CBO mean-field state is shown. We observe that the order parameter does not open a full gap, but significantly reduces the density of states at the Fermi level inducing two peaks above and below, in accordance with experimental findings [9,34,36–40].

Conclusion and outlook.—We have developed a minimal tight-binding model capturing the central features relevant for the discussion of charge density wave order in the kagome metals AV_3Sb_5. Motivated by recent experimental verification, we have investigated the motif of electronically driven charge order through a mean-field treatment of the kagome Hubbard model. Owing to the unique sublattice structure of the Fermi surface instability, a charge bond order with particle hole pairs of nonzero angular momentum emerges. From a Ginzburg Landau expansion of the free energy, we go beyond the instability level and find that the charge order in AV_3Sb_5 tends to yield orbital currents as a manifestation of time-reversal symmetry breaking, and is naturally prone to the onset of nematicity. The recently observed $2 \times 2 \times 2$ CDW in $(\mathrm{Rb}, \mathrm{Cs})V_3Sb_5$ [5,41] can likely be explained by extending the CBO order parameter in Eqs. (5) and (6) to three dimensions [42]. Intertwining these novel charge orders with the topological features of AV_3Sb_5 opens a phletora of exciting phenomena, in particular with respect to possibly highly exotic descendant superconducting pairing.

R. T. thanks S. A. Kivelson for discussions. This work is funded by the Deutsche Forschungsgemeinschaft (DFG, German Research Foundation) through Project-ID 258499086—SFB 1170 and through the Würzburg-Dresden Cluster of Excellence on Complexity and Topology in Quantum Matter—ct.qmat Project-ID 390858490—EXC 2147. Additionally, this project has received funding from the European Research Council (ERC) under the European Union's Horizon 2020 research and innovation programm (ERC-StG-Neupert-757867-PARATOP).

Note added.—Upon completion of this work, we became aware of Ref. [43] which investigates a slightly different charge bond order for AV_3Sb_5. Repeating our mean-field analysis for this order parameter yields a lower $k_B T_{\mathrm{CDW}} \approx 423$ meV (for $V = U = 1$ eV), rendering this order energetically less favorable.

[1] G. Grüner, Rev. Mod. Phys. **60**, 1129 (1988).
[2] L. P. Gor'kov and G. Grüner, *Charge Density Waves in Solids* (Elsevier, Amsterdam, 1989).
[3] B. R. Ortiz, L. C. Gomes, J. R. Morey, M. Winiarski, M. Bordelon, J. S. Mangum, I. W. H. Oswald, J. A. Rodriguez-Rivera, J. R. Neilson, S. D. Wilson, E. Ertekin, T. M. McQueen, and E. S. Toberer, Phys. Rev. Mater. **3**, 094407 (2019).
[4] Y.-X. Jiang *et al.*, Nat. Mater. **20**, 1353 (2021).
[5] H. X. Li, T. T. Zhang, Y. Y. Pai, C. Marvinney, A. Said, T. Yilmaz, Q. Yin, C. Gong, Z. Tu, E. Vescovo, R. G. Moore, S. Murakami, H. C. Lei, H. N. Lee, B. Lawrie, and H. Miao, Phys. Rev. X **11**, 031050 (2021).
[6] H. Chen *et al.*, arXiv:2103.09188.
[7] H. Zhao, H. Li, B. R. Ortiz, S. M. L. Teicher, T. Park, M. Ye, Z. Wang, L. Balents, S. D. Wilson, and I. Zeljkovic, arXiv:2103.03118.
[8] H. Tan, Y. Liu, Z. Wang, and B. Yan, Phys. Rev. Lett. **127**, 046401 (2021).
[9] E. Uykur, B. R. Ortiz, S. D. Wilson, M. Dressel, and A. A. Tsirlin, arXiv:2103.07912.
[10] F. Du, S. Luo, B. R. Ortiz, Y. Chen, W. Duan, D. Zhang, X. Lu, S. D. Wilson, Y. Song, and H. Yuan, Phys. Rev. B **103**, L220504 (2021).
[11] F. H. Yu, T. Wu, Z. Y. Wang, B. Lei, W. Z. Zhuo, J. J. Ying, and X. H. Chen, Phys. Rev. B **104**, 041103 (2021).
[12] Q. Yin, Z. Tu, C. Gong, Y. Fu, S. Yan, and H. Lei, Chin. Phys. Lett. **38**, 037403 (2021).
[13] M. L. Kiesel, C. Platt, and R. Thomale, Phys. Rev. Lett. **110**, 126405 (2013).
[14] W.-S. Wang, Z.-Z. Li, Y.-Y. Xiang, and Q.-H. Wang, Phys. Rev. B **87**, 115135 (2013).
[15] M. L. Kiesel and R. Thomale, Phys. Rev. B **86**, 121105(R) (2012).
[16] B. R. Ortiz, P. M. Sarte, E. M. Kenney, M. J. Graf, S. M. L. Teicher, R. Seshadri, and S. D. Wilson, Phys. Rev. Mater. **5**, 034801 (2021).
[17] B. R. Ortiz, S. M. L. Teicher, Y. Hu, J. L. Zuo, P. M. Sarte, E. C. Schueller, A. M. M. Abeykoon, M. J. Krogstad, S. Rosenkranz, R. Osborn, R. Seshadri, L. Balents, J. He, and S. D. Wilson, Phys. Rev. Lett. **125**, 247002 (2020).
[18] B. Bradlyn, L. Elcoro, J. Cano, M. G. Vergniory, Z. Wang, C. Felser, M. I. Aroyo, and B. A. Bernevig, Nature (London) **547**, 298 (2017).
[19] X. Wu, T. Schwemmer, T. Müller, A. Consiglio, G. Sangiovanni, D. D. Sante, Y. Iqbal, W. Hanke, A. P. Schnyder, M. M. Denner, M. H. Fischer, T. Neupert, and R. Thomale, Phys. Rev. Lett. **127**, 177001 2021.
[20] Y.-P. Lin and R. M. Nandkishore, Phys. Rev. B **100**, 085136 (2019).
[21] See Supplemental Material at http://link.aps.org/supplemental/10.1103/PhysRevLett.127.217601 for a discussion of m-type van-Hove singularities, pressure dependence of the results as well as details about the nematicity of the order parameter.
[22] X. Zhou, Y. Li, X. Fan, J. Hao, Y. Dai, Z. Wang, Y. Yao, and H.-H. Wen, Phys. Rev. B **104**, 041101 (2021).
[23] C. Nayak, Phys. Rev. B **62**, 4880 (2000).
[24] E. M. Kenney, B. R. Ortiz, C. Wang, S. D. Wilson, and M. Graf, J. Phys. Condens. Matter **33**, 235801 (2021).
[25] S.-Y. Yang, Y. Wang, B. R. Ortiz, D. Liu, J. Gayles, E. Derunova, R. Gonzalez-Hernandez, L. Šmejkal, Y. Chen, S. S. P. Parkin, S. D. Wilson, E. S. Toberer, T. McQueen, and M. N. Ali, Sci. Adv. **6**, eabb6003 (2020).

[26] A. A. Tsirlin, P. Fertey, B. R. Ortiz, B. Klis, V. Merkl, M. Dressel, S. D. Wilson, and E. Uykur, arXiv:2105.01397.
[27] Another CBO is discussed in Ref. [28], yielding the same critical temperature as obtained here.
[28] Y.-P. Lin and R. M. Nandkishore, Phys. Rev. B **104**, 045122 (2021).
[29] W. L. McMillan, Phys. Rev. B **12**, 1187 (1975).
[30] J. van Wezel, Europhys. Lett. **96**, 67011 (2011).
[31] Q. Liu, H. Yao, and T. Ma, Phys. Rev. B **82**, 045102 (2010).
[32] W. Zhu, S.-S. Gong, T.-S. Zeng, L. Fu, and D. N. Sheng, Phys. Rev. Lett. **117**, 096402 (2016).
[33] H. Li, H. Zhao, B. R. Ortiz, T. Park, M. Ye, L. Balents, Z. Wang, S. D. Wilson, and I. Zeljkovic, arXiv:2104.08209.
[34] N. Ratcliff, L. Hallett, B. R. Ortiz, S. D. Wilson, and J. W. Harter, arXiv:2104.10138.
[35] Z. X. Wang, Q. Wu, Q. W. Yin, C. S. Gong, Z. J. Tu, T. Lin, Q. M. Liu, L. Y. Shi, S. J. Zhang, D. Wu, H. C. Lei, T. Dong, and N. L. Wang, Phys. Rev. B **104**, 165110 (2021).
[36] S. Cho, H. Ma, W. Xia, Y. Yang, Z. Liu, Z. Huang, Z. Jiang, X. Lu, J. Liu, Z. Liu, J. Jia, Y. Guo, J. Liu, and D. Shen, arXiv:2105.05117.
[37] R. Lou, A. Fedorov, Q. Yin, A. Kuibarov, Z. Tu, C. Gong, E. F. Schwier, B. Büchner, H. Lei, and S. Borisenko, arXiv:2106.06497.
[38] Y. Hu, S. M. L. Teicher, B. R. Ortiz, Y. Luo, S. Peng, L. Huai, J. Z. Ma, N. C. Plumb, S. D. Wilson, J. F. He, and M. Shi, arXiv:2104.12725.
[39] K. Nakayama, Y. Li, M. Liu, Z. Wang, T. Takahashi, Y. Yao, and T. Sato, arXiv:2104.08042.
[40] Z. Wang, S. Ma, Y. Zhang, H. Yang, Z. Zhao, Y. Ou, Y. Zhu, S. Ni, Z. Lu, H. Chen, K. Jiang, L. Yu, Y. Zhang, X. Dong, J. Hu, H.-J. Gao, and Z. Zhao, arXiv:2104.05556.
[41] Z. Liang, X. Hou, W. Ma, F. Zhang, P. Wu, Z. Zhang, F. Yu, J. J. Ying, K. Jiang, L. Shan, Z. Wang, and X. H. Chen, Phys. Rev. X **11**, 031026 (2021).
[42] J. Ishioka, Y. H. Liu, K. Shimatake, T. Kurosawa, K. Ichimura, Y. Toda, M. Oda, and S. Tanda, Phys. Rev. Lett. **105**, 176401 (2010).
[43] X. Feng, K. Jiang, Z. Wang, and J. Hu, Sci. Bull. **66**, 1384 (2021).